Archives Italiennes de Biologie, 142: 511-523, 2004.

THE DYNAMICS OF SPINDLES AND EEG SLOW-WAVE ACTIVITY IN NREM SLEEP IN MICE

V.V. VYAZOVSKIY, P. ACHERMANN, A.A. BORBÉLY AND I. TOBLER[1]

Institute of Pharmacology and Toxicology, University of Zürich, Zürich, Switzerland

INTRODUCTION

In 1960 Michel Jouvet described the occurrence of spindles and slow waves in sleeping cats (12). These hallmarks of sleep, together with the EOG and EMG, provided the basis for the definition of sleep stages in non-human mammals (12, 13). The occurrence of spindles during sleep has been since described in most mammalian species. A comparison of the sleep EEG in mouse strains suggested that their occurrence is determined by genetic factors (28, 29). Neurophysiological mechanisms of spindle oscillations are intimately related to the generation of slow waves (23).

The temporal and spatial dynamics of slow-wave activity (SWA, EEG power between 0.5-4.0 Hz) and spindle activity during sleep could reflect complex regulatory processes. SWA is considered a marker of sleep homeostasis (6, 7), but little is known about the role of spindle activity in sleep regulation.

Spindles are generated within the reticular thalamic nuclei, where neurons typically exhibit a bursting discharge pattern at frequencies of 7-14 Hz in the cat (19) and the rat (15). The ensuing rhythmic hyperpolarisation of thalamocortical neurons leads to rebound spike bursts, which are transferred to the neocortex as spindles (20, 23). Whether thalamocortical bursts occur at delta- or spindle-frequencies depends on the level of membrane hyperpolarisation, which is influenced by activating cholinergic projections from the brainstem and basal forebrain (16, 17, 21). The incompatibility between spindles and delta waves occurs at the level of single neurons, but not necessarily in the EEG (23).

Several studies in humans report an inverse relationship between spindle-frequency activity (SFA, EEG power in the 12-15 Hz range) or spindle density and SWA (27, 2, 9, 31, 3, 14). It was shown that sleep deprivation (SD) not only leads to an increase in SWA, but to a concomitant decrease in SFA (5, 10) and spindle-density (9, 8, 14). A typical U-shaped distribution of SFA or spindle amplitude is observed within NREM sleep episodes (2, 9).

The data obtained in humans are supported by animal studies. In the rat EEG power between 10-25 Hz, increased progressively across the light period, whereas SWA showed an opposite trend (26). Furthermore, SD for 24 hours led to an increase

[1] Corresponding Author: Prof. Irene Tobler Ph.D., Institute of Pharmacology and Toxicology, University of Zurich, Winterthurerstr. 190 CH-8057 Zurich - Tel. +41 1 635 59 57 - Fax +41 1 635 57 07 - E-mail: tobler@pharma.unizh.ch

of SWA and a concomitant decrease of sigma activity (EEG power between 10-16 Hz) (18). At the transition from NREM sleep to REM sleep a pronounced increase of sigma activity occurred in rats (4, 26, 18) and several mouse strains (11, 32). These observations support the notion that spindles are hallmarks of "light" sleep (9, 23).

It is unknown whether EEG power in the sigma range is an adequate measure to quantify spindles in rodents, since spectral analysis does not allow to separate phasic spindle oscillations from continuous background EEG activity. Moreover, a quantitative assessment of spindles across 24 h or after prolonged waking in mice is lacking. We analyzed the occurrence of spindles and their relationship to spectral EEG power during a 24-h baseline as well as after 6 h SD in C57BL6 mice. We predicted that if spindles are a feature of "light" sleep, they would be reduced during recovery.

METHODS

Animals and surgery.

The experiments were performed according to the regulations of the local governmental commission for animal research. Recordings were obtained in adult male C57BL/6J mice (n = 7), 17.5 weeks ± 0.1 SEM old and weighing 27.2 g ± 1.1 at surgery. The mice were kept individually in Macrolon cages (36 x 20 x 35 cm) with food and water available ad libitum, and maintained in a 12-h light-12-h dark cycle (light from 8.00-20.00 h; 7 Watt OSRAM Dulux EL energy saving lamp, approximately 30 lux). Mean ambient temperature was 23.0 ± 0.2 °C. Under deep equithesin (pentobarbital/chloral hydrate) anaesthesia (0.4 ml/100 g, i.p.) the mice were implanted with gold-plated, round-tipped miniature screws (0.9 mm diameter) that served as EEG electrodes. The epidural electrodes were placed bilaterally over the parietal cortex (3 mm lateral to midline, 2 mm posterior to bregma) and frontal cortex (1.5 mm lateral to midline and 1.5 mm anterior to bregma). The common reference electrode was placed above the cerebellum (2 mm posterior to lambda, on midline). Two gold wires (diameter 0.2 mm) inserted into the neck muscles served to record the electromyogram (EMG). The electrodes were connected to stainless steel wires that were fixed to the skull with dental cement. At least 3 weeks were allowed for recovery after surgery and adaptation to the recording conditions.

Experimental protocol, data acquisition and analysis.

The EEG and EMG were recorded continuously for 48 h. A 24-h baseline preceded the 6-h sleep deprivation (SD) starting at light onset. The SD performed by gentle handling as previously (25) was effective, since only 3.11 min ± 1.2 of NREM sleep occurred during the 6-h SD period. The EEG and EMG signals were amplified (amplification factor approx. 2,000), conditioned by analogue filters (high-pass filter: -3 dB at 0.016 Hz; low-pass filter: -3 dB at 40 Hz, less than -35 dB at 128 Hz) sampled with 512 Hz, digitally filtered (EEG: low-pass FIR filter 25 Hz; EMG: band-pass FIR filter 20-50 Hz) and stored with a resolution of 128 Hz. Ambient temperature within the cage was sampled at 4-s intervals. The three vigilance states NREM sleep, REM sleep and waking were determined for 4-s epochs by visual inspection of the parietal EEG and EMG records and the values of SWA (25). Epochs containing EEG artifacts in any one of the four derivations were excluded from spectral analyses in all derivations (excluded epochs as % of recording time: waking: 38.7 ± 6.8; NREM sleep: 2.7 ± 0.7; REM sleep: 1.5 ± 0.3). EEG power spectra were computed for 2-s epochs by a fast Fourier transform routine (Hanning window). Interhemispheric EEG coherence spectra were computed between left and right bipolar fronto-parietal derivations for consecutive 12-s epochs (six 2-s epochs) (30). Frequency resolution of power and coherence spectra was 0.5 Hz.

Spindle analysis.

Inspection of the raw EEG allowed the visual recognition of spindle events in the frontal derivations (Fig. 1). Preliminary spectral analysis of 4-s epochs with spindles showed a peak at 10-13 Hz. Therefore the EEG was band pass filtered between 10-13 Hz (Fig. 1), and an algorithm was developed for automatic detection of spindles in the filtered signal. An upper and a lower ("noise") threshold was determined for each mouse. A spindle was detected by the algorithm when the upper threshold was exceeded, and its beginning and ending was defined as the point when the filtered signal exceeded and fell below the "noise" level, respectively. In addition, to account for the waxing and waning of the filtered signal (e.g. Fig. 1, spindle #3) an individually determined maximal interruption within a spindle was allowed. To validate the performance of the algorithm in NREM sleep, the first 1-h interval after light onset was analysed automatically and compared with visually scored spindles (visual vs algorithm: mean difference 5.9% ± 1.0; $p = 0.3$, paired t-test, $n = 7$).

Spindle density was defined as the number of spindles (i.e. midpoints of spindles) per 1 h of NREM sleep, REM sleep or waking.

For signal analysis the software package MATLAB (The Math Works, Inc., Natick, MA, USA) was used and statistical analysis was performed with SAS (SAS Institute, Inc., Cary, NC, USA).

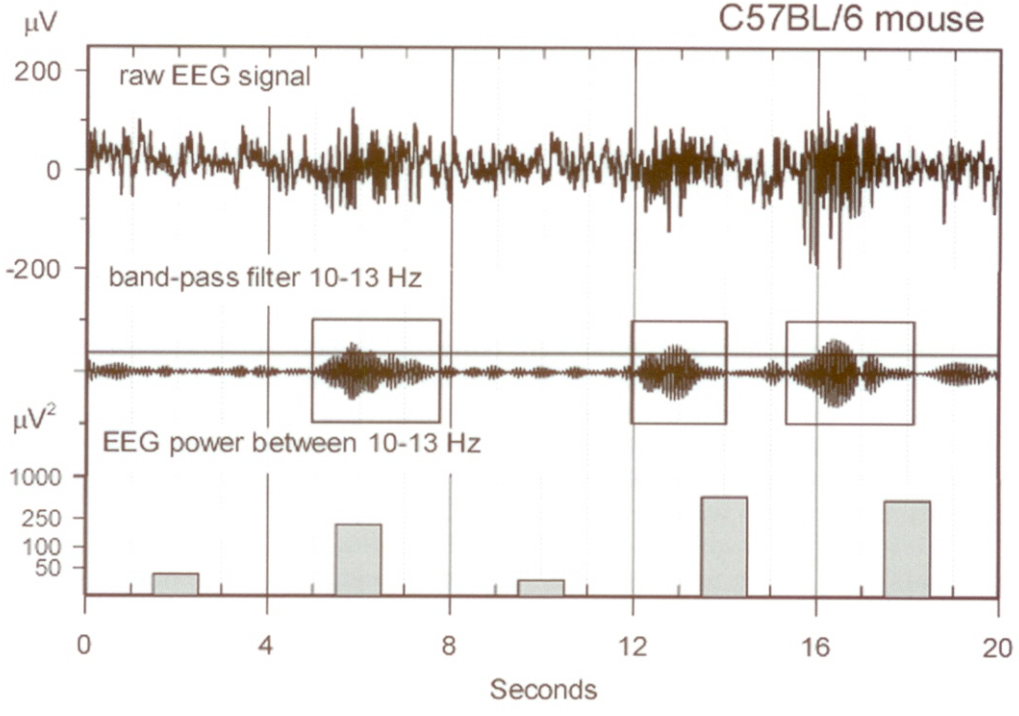

Fig. 1. *Example of a 20-s raw EEG record of NREM sleep from the right frontal derivation with three visually detected spindles.*

Middle: corresponding band-pass filtered EEG (10-13 Hz, 4th order Chebyshev type II filter, forward and reverse filtering). Three spindle events detected by the algorithm are shown on the filtered signal. Horizontal line shows upper threshold level. Bars: EEG power between 10-13 Hz of corresponding 4-s epochs (log scale).

RESULTS

Spindle-events detected in the right frontal derivation occurred predominantly during NREM sleep or at the NREM-REM sleep transition (Tab. I). Since spindle density in REM sleep was 5.8 times lower than in NREM sleep, and only few spindles occurred during waking, analysis was restricted to NREM sleep spindles.

Tab. I. *Absolute number of spindles detected in individual mice during the 24-h baseline (24 h), and spindle density (n/1 h) in NREM sleep, waking and REM sleep.*
NREM sleep spindles are subdivided into those occurring during the last 32 s before the transition to REM sleep (N-R spindles) and remaining spindles (N-spindles). All NREM sleep spindles were pooled for statistical comparisons. Mean values ± SEM (n = 7; epochs with artifacts excluded). Letters indicate significant differences between corresponding values (24-h or n/1 h) ([a] N-spindles vs N-R spindles, $p < 0.001$; [b] N-spindles vs N-R spindles, $p < 0.01$; [c] all NREMS spindless vs REMS; [d] all NREMS spindles vs waking, $p < 0.001$; [e] waking vs REMS, $p < 0.01$, paired t-test).

	N - spindles		N-R transition spindles		REM sleep spindles		Waking spindles	
Mouse #	24 h	n/1 h	24 h	n/1 h	24 h	n/1 h	24 h	n/1 h
1	1994	243.6	189	276.1	40	35.1	35	6.0
2	2520	265.4	259	331.1	78	47.5	24	2.5
3	2244	272.6	299	336.4	77	56.2	33	4.2
4	1822	239.2	257	332.3	73	51.5	27	3.5
5	1899	207.4	152	300.0	23	19.4	6	0.9
6	1985	269.7	286	346.0	81	48.9	48	3.7
7	1879	262.5	249	341.6	88	62.7	37	4.5
Mean	2049.0 ± 93.8	251.5 ± 8.8	241.6 ± 19.9[a]	323.4 ± 9.7[b]	65.7 ± 9.2[c]	45.9 ± 5.5[c]	30 ± 4.9[d,e]	3.6 ± 0.6[d,e]

Spindles in the frontal derivation were observed visually simultaneously in the left and right hemisphere. To assess their relationship, interhemispheric EEG coherence spectra were computed between the left and right bipolar (fronto-parietal) derivations. Interhemispheric coherence of those 12-s epochs in NREM sleep where spindles were detected by the algorithm was significantly higher between 10-12.5 Hz compared to epochs without spindles (Fig. 2).

To investigate the frequency composition of spindles, EEG power spectra were computed for 2-s epochs identified as ± 1 s from the midpoints of spindles and compared with the remaining 2-s epochs without spindles. The occurrence of spindles led to a prominent peak of EEG power within the sigma-frequency range (Fig. 3). The peak during epochs with spindles occurred at 11.1 ± 0.1 Hz (n = 7). EEG power of epochs with spindles exceeded power of epochs without spindles in all frequency bins above 4.5 Hz. Corresponding EEG spectra of the parietal derivation showed a smaller difference. Interaction of factors 'derivation' (frontal, parietal) x 'spindle occurrence' (epochs with and without spindles) was significant between 7.0-25.0 Hz ($p < 0.05$, 2-way ANOVA).

To further investigate the relationship between spindles and the power spectrum, the time course of spindle occurrence (n/4 s) and corresponding 4-s spectral values

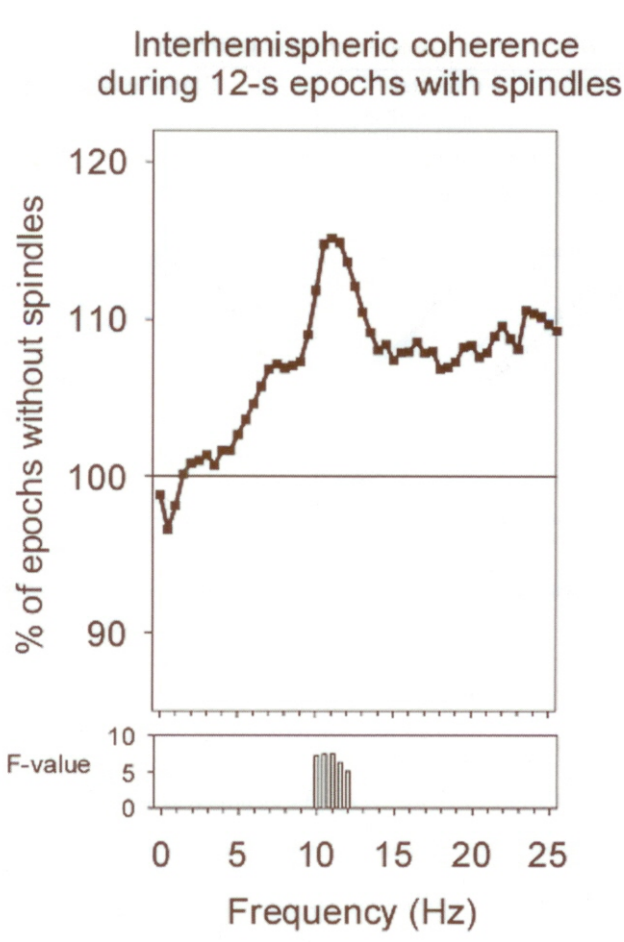

Fig. 2. *Interhemispheric EEG coherence spectrum in NREM sleep computed for 12-s epochs of the 24-h baseline.*

Left-right coherence between epochs where spindles were detected in the right frontal derivation (1448.9 ± 62.4 epochs) is represented as percentage of coherence computed for the remaining epochs without spindles (1169.6 ± 60.5 epochs) = 100%. Mean values (n = 7) are shown. Vertical bars in the lower panel represent bins with significant F-values (one-way ANOVA on Fisher's z-transformed coherence values; $p < 0.05$, comparison of epochs with and without spindles).

were computed for transitions from waking or REM sleep to NREM sleep and NREM sleep to REM sleep (Figs. 4, 5). An increase of EEG power in frequencies below 10 Hz occurred immediately after the transition to NREM sleep in the parietal derivation, while the increase was more gradual in the frontal derivation. A selective enhancement of EEG power within the sigma range was evident prior to the transition to REM sleep in the frontal derivation only (Fig. 4, upper right panel). EEG spectra of the parietal derivation were characterized by a marked

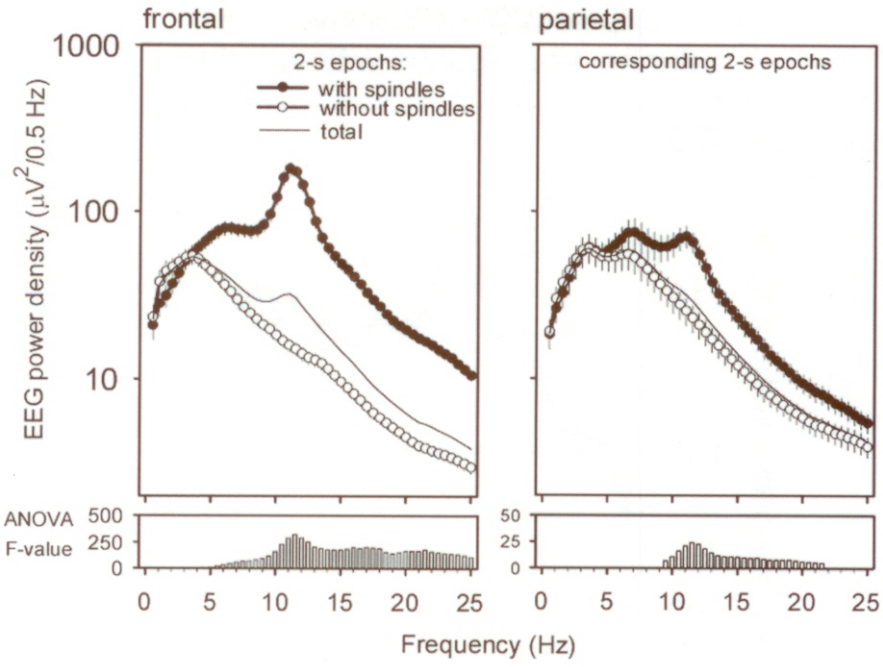

Fig. 3. *EEG power spectra in NREM sleep for the 24-h baseline for the right frontal and parietal derivation.*

Mean EEG spectra (n = 7, C57BL/6 mice) for 2-s epochs identified as ± 1 s from the midpoints of spindles (2259.6 ± 101.7 epochs), epochs without spindles (11271.4 ± 434.0 epochs) and for all 2-s epochs in NREM sleep (total = 17239.4 ± 561.7 epochs). Vertical bars in the lower panels represent bins with significant F-values for the comparison between epochs with spindles and without spindles (1-way ANOVA on log-transformed values, $p < 0.05$).

increase of EEG power within the theta-range (6-9 Hz) after the transition to REM sleep (Fig. 4).

The number of spindles increased within the first 20 s after the transition from waking or REM sleep to NREM sleep (Fig. 5). A second surge was apparent in the last 30 s of NREM sleep before the transition to REM sleep. SWA showed a concomitant increase at the beginning of the NREM sleep episode, whereas in contrast to spindles, the SWA decline began approximately 30 s before the transition to REM sleep (Fig. 5, right lower panel).

The 24-h time course of spindle density (n/1 h of NREM sleep) and SWA in NREM sleep is illustrated in Figure 6. Spindle density increased in the course of the light period and decreased progressively after dark onset reaching a minimum in the middle of the dark period (Fig. 6, upper panel), whereas SWA showed an opposite evolution (Fig. 6, lower panel).

Spindle duration during baseline was 1.8 s ± 0.03 (mean of individual median values, n = 7). To investigate changes in spindle consolidation across 24 h, the time

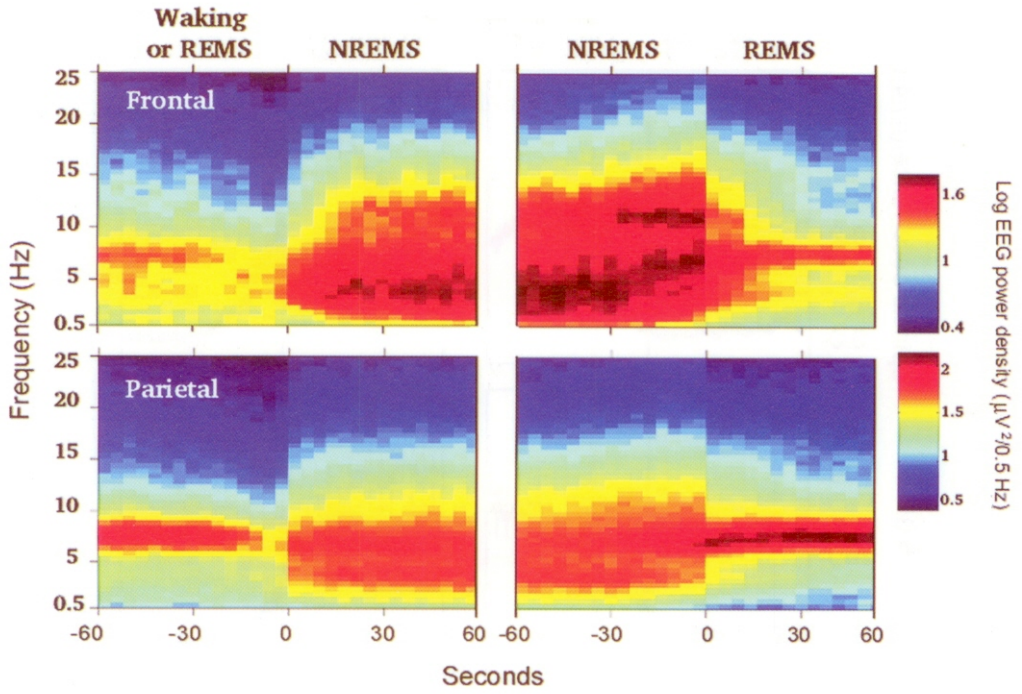

Fig. 4. *Dynamics of EEG spectra are shown for the transition from waking or REM sleep to NREM sleep and from NREM sleep to REM sleep for the 24-h baseline (48.0 ± 2.0 episodes per animal).*

The minute prior and after the transition (= 0) is illustrated based on 4-s epochs (x-axis: in seconds). First and last minute of the same NREM sleep episode is shown. Episodes longer than 2 min were selected, allowing interruptions of maximum 12 s REM sleep or 40 s waking. Waking or REM sleep could precede the episode. Mean values (n = 7) for the frontal (top panels) and parietal (lower panels) derivation. EEG power density is color-coded according to the scale on the right.

course of spindle duration and standard deviation of intra-spindle amplitude was computed. Neither spindle duration nor the standard deviation of intra-spindle amplitude showed significant changes within the light or dark period (1-way ANOVA for repeated measures, factor "2-h interval"). Both these variables were significantly higher in the light period than in the dark period ($p < 0.05$; paired t-test, data not shown).

Based on the results depicted in the upper panel of Figure 5, spindle density was computed separately for spindles occurring during the last 32 seconds of a NREM sleep episode before the transition to REM sleep (N-R spindles) and the remaining NREM sleep spindles (N-spindles). The power spectra of N-spindles and N-R spindles did not differ (not shown), and the peak frequency in the power spectra of N- and N-R spindles was similar (11.1 ± 0.1 and 11.0 ± 0.1 Hz respectively; $p = 0.4$, paired t-test).

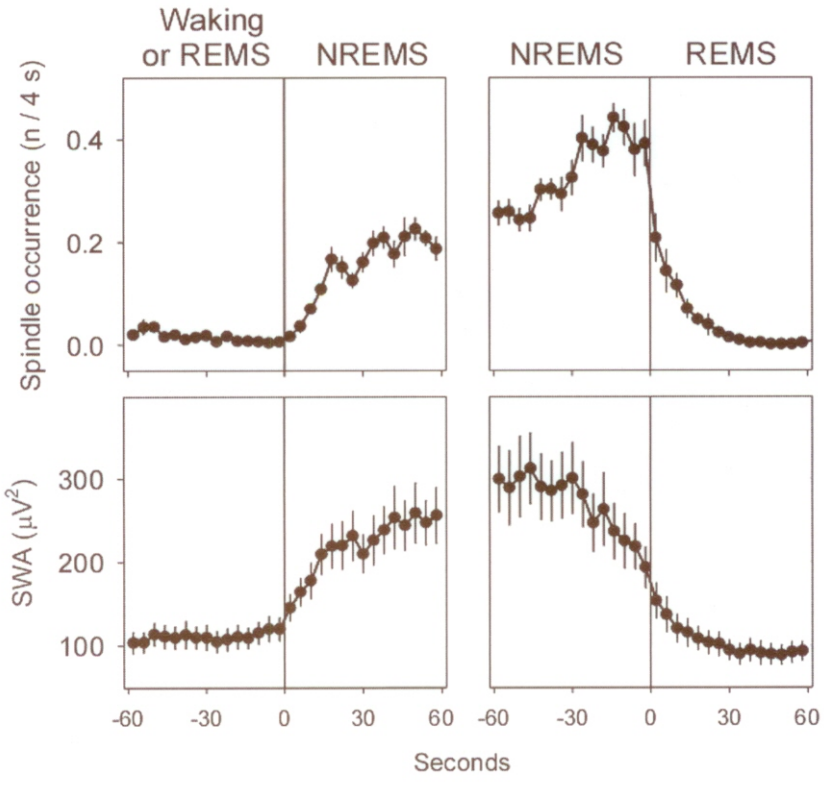

Fig. 5. *Dynamics of spindle occurrence (number of midpoints of spindles per 4-s epoch) and slow wave activity (SWA; EEG power in 0.5-4.0 Hz range) in the frontal derivation during the transition from waking or REM sleep to NREM sleep (left panels) and from NREM sleep to REM sleep (right panels) for the 24-h baseline.*

The minute prior and after the transition (= 0) is illustrated based on the mean of 4-s epochs (n = 7, C57BL/6 mice). The same criteria for selection of NREM sleep episodes were applied as in Figure 4. First and last minute of the same NREM sleep episodes is shown as in Figure 4.

During the light period N-spindles showed an opposite time course to that of N-R spindles (Fig. 7). Sleep deprivation had a clear effect on both types of spindles. During recovery N-spindle density was initially reduced, and enhanced towards the middle of the dark period [Fig. 7, upper panel; interaction in 2-way ANOVA, factors 'day (baseline, recovery)' x '2-h interval': $p < 0.05$]. The increase computed for the entire 12-h dark period was significant ($p < 0.01$). In contrast, N-R spindle density was enhanced only in the first 2 h after SD [Fig. 7, lower panel; $p < 0.05$, paired t-test, after significant interaction in 2-way ANOVA, factors 'day (baseline, recovery)' x '2-h interval' (only for the light period)]. The number of NREM-REM sleep transitions during the first 2 h after SD did not differ from the corresponding baseline value (baseline: 12.3 ± 1.6; recovery: 14.9 ± 2.0; $p = 0.3$, paired t-test).

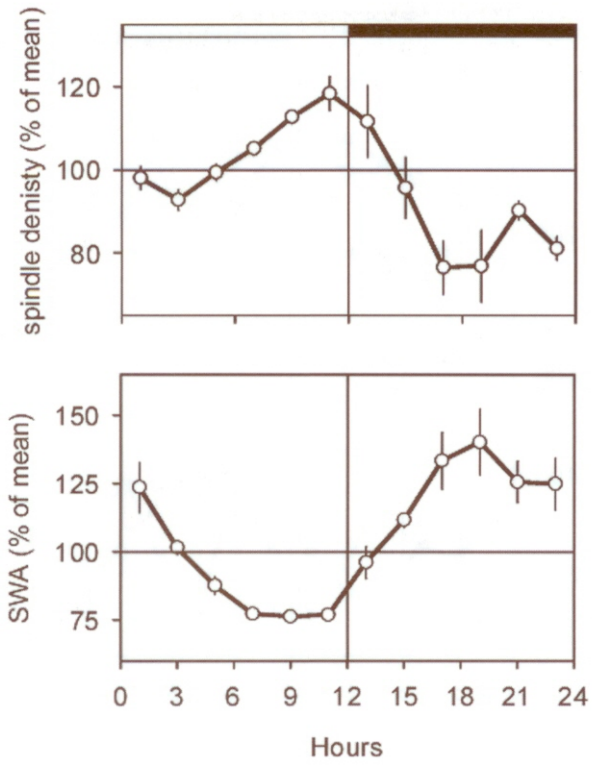

Fig. 6. *Time course of spindle density (number of spindles per 1 h of NREM sleep) and slow wave activity (SWA, EEG power between 0.5-4 Hz) in NREM sleep in the right frontal derivation during 24 h baseline.*

Upper panel: spindle density; lower panel: SWA. Relative values (% of 24-h mean; n = 7 ± SEM) are shown for 2-h intervals.

The time course of the peak in the power spectrum within the 10-13 Hz range computed for the frontal derivation for all 2-s epochs with spindles was unchanged in the first three 2-h intervals after SD. In the dark period peak frequency was enhanced in the first and fifth 2-h interval (paired t-test, after significant ANOVA, factor 'day', $p < 0.0001$, not shown).

DISCUSSION

This study is the first quantitative assessment of sleep spindles across 24 h and after sleep deprivation in mice. Spindles were evident in the frontal derivation where they led to a prominent peak in the EEG spectrum with a maximum close to 11 Hz.

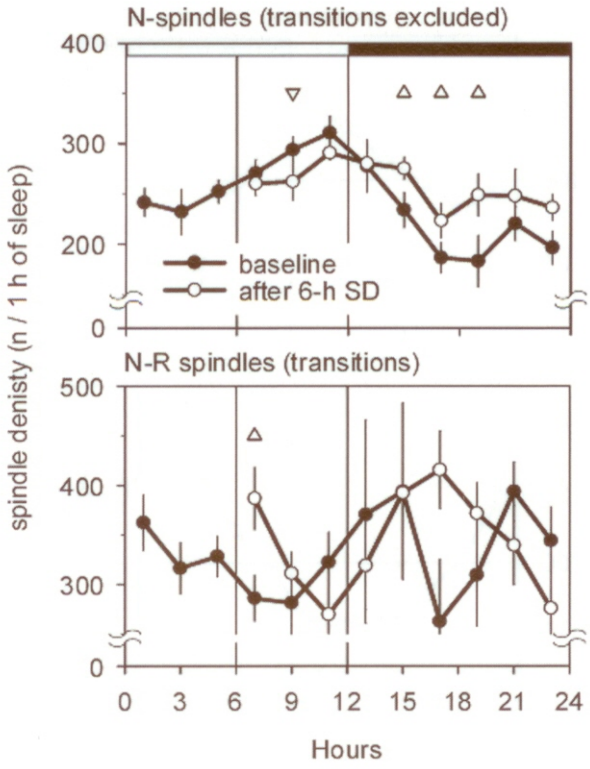

Fig. 7. *Time course of spindle density (number of spindles per 1 h of NREM sleep) in the right frontal derivation.*

Upper panel: N-spindles, lower panel: N-R spindles. Mean values (n = 7) ± SEM are shown for 2-h intervals during the 24-h baseline and 18 h recovery after 6 h sleep deprivation (SD). Triangles indicate significant change after SD ($p < 0.05$, paired t-test after significant interaction in 2-way ANOVA, factors 'day (baseline, recovery)' x '2-h interval').

This frontal predominance in spindle occurrence may be a consequence of morphological differences between the neocortical areas, or it may be due to an anterior-posterior gradient in thalamocortical projections. Spindles occurring throughout NREM sleep (N-spindles) and those occurring before transitions from NREM sleep to REM sleep likely originate from the same source, because their predominant frequency was identical.

The increased interhemispheric coherence between 10-12.5 Hz during epochs with spindles is consistent with the prominent coherence peak in 13-14 Hz in humans (1). This synchronisation could be mediated by direct connections between the left and right reticular nuclei (24). In addition, there is evidence in acallosal mice that the corpus callosum is important for interhemispheric synchronization of the EEG during sleep (30).

There was a complex relationship between spindles and SWA in NREM sleep. Our data show that oscillations at delta and spindle frequencies can coexist at the EEG level, because both measures increased concomitantly at the beginning of NREM sleep episodes. However, an inverse relationship between SWA and spindles prior to the transition to REM sleep may indicate that spindles are facilitated when SWA is low, or that the mechanisms governing the occurrence of spindles differ in NREM sleep immediately preceding REM sleep from the other part of the NREM sleep episode.

The notion that spindles are increased when SWA is low is supported also by the opposite evolution of SWA and spindle density during 24 h. However, this time course may be determined not only by homeostatic sleep pressure, but also by circadian influences. Thus, spindles progressively increased in the second half of the light period reaching a maximum during the last 2-h interval, while SWA was at its lowest level, and did not show variations. Similarly, in humans the most pronounced increase of spindle-frequency activity (EEG power in the 12-15 Hz range) occurred after prolonged sleep (3).

To further investigate the effects of increased sleep pressure, spindles were analyzed after 6-h SD. As expected, N-spindle density was initially lowered, while SWA showed a well-known increase. Subsequently, the delayed increase of N-spindles coincided with a negative rebound of SWA during the dark period. These results may indicate that N-spindles reflect sleep maintenance processes (33), opposing decreased homeostatic sleep pressure, or the circadian drive for wakefulness. In support of this interpretation, an enhancement of NREM sleep after SD was also most pronounced in the dark period.

In contrast to N-spindles, N-R spindles were enhanced only in the first 2 h after SD. This increase could be compensatory, because SWA prior to the transition to REM sleep is lower and would not prevent spindle occurrence. Alternatively, the increased spindle density prior to the transitions to REM sleep may be a manifestation of increased REM sleep propensity after SD, when the rebound of REM sleep is not yet expressed.

SUMMARY

A quantitative analysis of spindles and spindle-related EEG activity was performed in C57BL/6 mice. The hypothesis that spindles are involved in sleep regulatory mechanisms was tested by investigating their occurrence during 24 h and after 6 h sleep deprivation (SD; n = 7).

In the frontal derivation distinct spindle events were characterized as EEG oscillations with a dominant frequency approximately at 11 Hz. Spindles were most prominent during NREM sleep and increased before NREM-REM sleep transitions. Whereas spindles increased concomitantly with slow wave activity (SWA, EEG power between 0.5 and 4.0 Hz) at the beginning of the NREM sleep episode, these measures showed an opposite evolution prior to the transition to REM sleep.

The 24-h time course of spindles showed a maximum at the end of the 12-h light period, and was a mirror image of SWA in NREM sleep. After 6 h SD the spindles in NREM sleep were initially suppressed, and showed a delayed rebound. In contrast, spindles occurring immediately before the transition to REM sleep were enhanced during the first 2 h of recovery. The data suggest that spindles in NREM sleep may be involved in sleep maintenance, while spindles heralding the transition to REM sleep may be related to mechanisms of REM sleep initiation.

Acknowledgements. - Supported by the: Swiss National Science Foundation grants 3100-053005.97 and 3100A0-100567 and Human Frontier Science Program RG00131/2000

REFERENCES

1. ACHERMANN, P. AND BORBÉLY, A.A. Coherence analysis of the human sleep electroencephalogram. *Neuroscience*, **85:** 1195-1208, 1998.
2. AESCHBACH, D. AND BORBÉLY, A.A. All-night dynamics of the human sleep EEG. *J. Sleep Res.*, **2:** 70-81, 1993.
3. AESCHBACH, D., DIJK, D.J. AND BORBÉLY, A.A. Dynamics of EEG spindle frequency activity during extended sleep in humans: relationship to slow-wave activity and time of day. *Brain Res.*, **748:** 131-136, 1997.
4. BENINGTON, J.H., KODAL, S.K. AND HELLER, H.C. Scoring transitions to REM sleep in rats based on the EEG phenomena of pre-REM sleep: an improved analysis of sleep structure. *Sleep,* **17:** 28-36, 1994.
5. BORBÉLY, A.A., BAUMANN, F., BRANDEIS, D., STRAUCH, I. AND LEHMANN, D. Sleep deprivation: effect on sleep stages and EEG power density in man. *Electroencephalogr. Clin. Neurophysiol.,* **51:** 483-495, 1981.
6. BORBÉLY, A.A. A two process model of sleep regulation. *Hum. Neurobiol.,* **1:** 195-204, 1982.
7. BORBÉLY, A.A. AND ACHERMANN, P. Homeostasis of human sleep and models of sleep regulation. Pp 377-390. In: KRYGER M.H., ROTH T. AND DEMENT, W.C. (Eds) *Principles and Practice of Sleep Medicine*. W.B. Saunders Co., Philadelphia, 2000.
8. DE GENNARO, L., FERRARA, M. AND BERTINI, M. Topographical distribution of spindles: variations between and within NREM sleep cycles. *Sleep Res. Online,* **3:** 155-160, 2000.
9. DIJK, D.J., HAYES, B. AND CZEISLER, C.A. Dynamics of electroencephalographic sleep spindles and slow wave activity in men: effect of sleep deprivation. *Brain Res.,* **626:** 190-199, 1993.
10. FINELLI, L.A., BORBÉLY, A.A. AND ACHERMANN, P. Functional topography of the human nonREM sleep electroencephalogram. *Eur. J. Neurosci.,* **13:** 2282-2290, 2001.
11. FRANKEN, P., MALAFOSSE, A. AND TAFTI, M. Genetic variation in EEG activity during sleep in inbred mice. *Am. J. Physiol.,* **275:** R1127-1137, 1998.
12. JOUVET, M., MICHEL, F. AND MOUNIER, D. Analyse électroencéphalographique comparée du sommeil physiologique chez le chat et chez l'homme. *Rev. Neurol., Paris,* **103:** 189-205, 1960.
13. JOUVET, M. The states of sleep. *Sci. Am.,* **216:** 62-68, 1967.
14. KNOBLAUCH, V., MARTENS, W.L., WIRZ-JUSTICE, A. AND CAJOCHEN, C. Human sleep spindle characteristics after sleep deprivation. *Clin. Neurophysiol.,* **114:** 2258-2267, 2003.
15. MARKS, G.A. AND ROFFWARG, H.P. Spontaneous activity in the thalamic reticular nucleus during the sleep/wake cycle of the freely-moving rat. *Brain Res.,* **623:** 241-248, 1993.

16. PARÉNT, A., PARÉ, D., SMITH, Y. AND STERIADE, M. Basal forebrain cholinergic and non-cholinergic projections to the thalamus and brainstem in cats and monkeys. *J. Comp. Neurol.*, **277:** 281-301, 1988.
17. PARE, D., SMITH, Y., PARÉNT, A. AND STERIADE, M. Projections of brainstem core cholinergic and non-cholinergic neurons of cat to intralaminar and reticular thalamic nuclei. *Neuroscience,* **25:** 69-86, 1988.
18. SCHWIERIN, B., ACHERMANN, P., DEBOER, T., OLEKSENKO, A., BORBÉLY, A.A. AND TOBLER, I. Regional differences in the dynamics of the cortical EEG in the rat after sleep deprivation. *Clin. Neurophysiol.*, **110:** 869-875, 1999.
19. STERIADE, M., DOMICH, L. AND OAKSON, G. Reticularis thalami neurons revisited: activity changes during shifts in states of vigilance. *J. Neurosci.*, **6:** 68-81, 1986.
20. STERIADE, M., GLOOR, P., LLINÁS, R.R., LOPES DE SILVA, F.H. AND MESULAM, M.M. Report of IFCN Committee on Basic Mechanisms. Basic mechanisms of cerebral rhythmic activities. *Electroencephalogr. Clin. Neurophysiol.*, **76:** 481-508, 1990.
21. STERIADE, M. AND AMZICA, F. Coalescence of sleep rhythms and their chronology in corticothalamic networks. *Sleep Res. Online,* **1:** 1-10, 1998.
22. STERIADE, M., DATTA, S., PARÉ, D., OAKSON, G. AND CURRO DOSSI, R.C. Neuronal activities in brain-stem cholinergic nuclei related to tonic activation processes in thalamocortical systems. *J. Neurosci.*, **10:** 2541-2559, 1990.
23. STERIADE, M. The corticothalamic system in sleep. *Frontiers in Biosciences,* **8:** d878-d899, 2003.
24. TIMOFEEV, I. AND STERIADE, M. Low-frequency rhythms in the thalamus of intact-cortex and decorticated cats. *J. Neurophysiol.*, **76:** 4152-4168, 1996.
25. TOBLER, I., DEBOER, T. AND FISCHER, M. Sleep and sleep regulation in normal and prion protein-deficient mice. *J. Neurosci.*, **17:** 1869-1879, 1997.
26. TRACHSEL, L., TOBLER, I. AND BORBÉLY, A.A. Electroencephalogram analysis of non-rapid eye movement sleep in rats. *Am. J. Physiol.*, **255:** R27-37, 1988.
27. UCHIDA, S., MALONEY, T., MARCH, J.D., AZARI, R. AND FEINBERG, I. Sigma (12-15 Hz) and delta (0.3-3 Hz) EEG oscillate reciprocally within NREM sleep. *Brain Res. Bull.*, **27:** 93-96, 1991.
28. VALATX, J.L. Enregistrement chronique des activités électriques cérébrales, musculaires et oculaires chez la Souris. *C. R. Seances Soc. Biol. Fil.*, **165:** 112-115, 1971.
29. VALATX, J.L., BUGAT, R. AND JOUVET, M. Genetic studies of sleep in mice. *Nature,* **238:** 226-227, 1972
30. VYAZOVSKIY, V., ACHERMANN, P., BORBÉLY, A.A. AND TOBLER, I. Interhemispheric coherence of the sleep EEG in mice with congenital callosal dysgenesis. *Neuroscience,* **124:** 481-488, 2004.
31. WERTH, E., ACHERMANN, P., DIJK, D.J. AND BORBÉLY, A.A. Spindle frequency activity in the sleep EEG: individual differences and topographic distribution. *Electroencephalogr. Clin. Neurophysiol.*, **103:** 535-542, 1997.
32. WISOR, J.P., DELOREY, T.M., HOMANICS, G.E. AND EDGAR, D.M. Sleep states and sleep electroencephalographic spectral power in mice lacking the beta 3 subunit of the GABA(A) receptor. *Brain Res.*, **955:** 221-228, 2002.
33. YAMADORI, A. Role of the spindles in the onset of sleep. *Kobe J. Med. Sci.*, **17**: 97-111, 1971.